Journal of Natural Sciences Research www.iiste.org
ISSN 2224-3186 (Paper) ISSN 2225-0921 (Online)
Vol.5, No.15, 2015

Effect of Boundary/Wall Material of the Shape of Thermal Neutron Flux Pattern

NWOSU, O.B
Department of Physics and Industrial Physics, Faculty of physical sciences, Nnamdi Azikiwe University Awka, Anambra state, Nigeria

Abstract.
An In-115 foils activated at various distances from the centred Pu/Be neutron source in a polythene walled neutron water tank at Manchester labouratory; and an MCNP code simulation with a polythene wall and a stainless steel wall has been used to study neutron flux distribution pattern and the effect of the wall material on this flux pattern. Four he-3 detectors was modelled using MCNP codes to have been inserted; first into a polythene walled neutron tank at different distances from the source to study how thermal neutrons distribute themselves across the diameter of the tank. Again it was remodelled changing the wall from polythene to a stainless steel to observe the wall effect on the flux pattern. It was discovered that thermal flux in both walls generally have a dume shaped curve with definite maximum at the center and tending to zero at the edge seemingly obeying the Fick's law and the diffusion theory. The polythene walled neutron tank experiment and it's simulation exhibited same flux pattern but with little rise in flux towards the polythene wall before finally droping off to zero, while there was no such rise at the edges of the stainless steel walled tank. These two different behavious could be likened to reflected and bare core reactor, where the polythene because of its property thermalzed and reflect back some fast escaping neutron leading to such little rise in flux at the edges unlike the stainless steel which does not. This thermal flux pattern reveals power level distribution in the reactor core and has led to the theory of diffenrential enrichment, enriching fuel at the edges higher than those at the centre to balance thermal flux deficiency at the edges and sufficiency at the centre. Core with reflector will ensure maximum utilization of fuel.

1.0 Introduction:

Activation experiment is one of the methods employed in neutron flux detection. Usually an activation foils could be inserted at different distances in a rector core and made radioactive, and the emmited gamma ray counted using gamma ray detector. An Indium-115 foil was inserted at different distances from the centered Pu-Be neutron source in a polythene walled neutron tank to tally the flux pattern within the tank. Using He-3 detector or BF-3 detector is yet another way of tallying for neutron flux. Four He-3 detector was modelled using MCNP codes to have been inserted at various distances from the Pu-Be neutron source. First a polythene wallled neutron tank was assumed and later remodelled using a stainless steel wall in order to observe if these two types of wall will have any effect on the flux distribution pattern. Different theories like Fick`s law, Diffusion law, Boltzmann equation etc has given insight into neutron distribution behaviour in a scatterring and non absorbing medium and this work has equaly tested the validity of these theories.

1.1 The Fick's Law and Diffusion law

This theory is widely used in nuclear reactor analysis and makes accurate predictions of thermal neutron flux distribution. Neutron's diffusion pattern like that of gas has been shown {1,4}as diffusing from a region of higher density to a region of lower density (fig1.0) under the conditions; that the neutron scattering is isotropic, that there is no source of neutrons or boundary nearby, and that the medium is not strongly neutron absorbing.

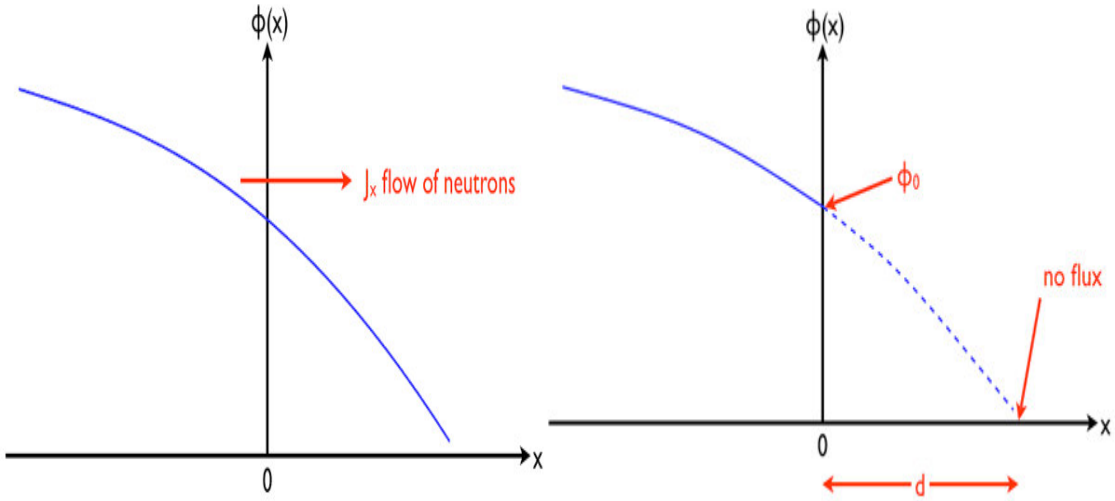

Fig1.0 Movement of neutrons from a region of high density to low density to flatten the gradient (Fick's Law in one dimension); Maximum flux at the centre and zero flux at the end point {1,4}

Under these conditions, the Fick's law of neutron diffusion relates the neutron current density vector J (r,v,t) to the neutron flux φ(r, v, t), stating that the net rate of neutron flow in a given direction is proportional to the negative spatial gradient of the neutron flux *{1}*

Fick's law stated mathematically shows that

$$J_z = -D\frac{d\phi}{dz}$$ (in 1-dimension, Z) ……1.0

J_z = -D gradϕ = -D$\nabla\phi$ (in 3-dimension)

Where gradϕ is the neutron flux gradient in z direction; J_z is the neutron current density (n/sec.cm$^{2)}$ and D is the neutron current Diffusion coefficient (cm) = $D = \frac{\lambda_{TR}}{3} = \frac{1}{3\sum_{TR}}$ ∇ is the gradient operator

Inserting this Fick's law of equation 1.0 into the leakage term in a general one-speed neutron balance (the neutron conservation equation) given as

$$s(r,t) - \sum_a \phi(r,t) - \nabla.J(r,t) = \frac{\partial n(r,t)}{\partial t}$$ ……2.0

ie (source –absorption – leakage = net rate of change of neutron density) gives the neutron diffusion equation as

$$\phi(r,t)] - \sum_a \phi(r,t) + S(r,t) = \frac{\partial n(r,t)}{\partial t}$$ ……3.0

For a system in a steady state, like, the critical reactor, $\frac{\partial n}{\partial t} = 0$;

The steady state for one dimensional diffusion equation according to Samuel and Alexander, 1981 becomes

$$D\nabla^2\phi(r,t)] - \sum_a \phi(r,t) + S(r,t) = 0;$$ ……4.0

When we divide the above by ∑ so that D/∑ appears, then the square-root of this has been termed as the neutron diffusion length (L= (D/∑)$^{1/2}$).

1.2 The Neutron Boltzmann equation and the Maxwellian–Boltzmann distributions.

The neutron Boltzmann equation, also called the neutron transport equation describes neutron behaviours like scattering and absorption, in a medium filled with nuclei like the nuclear reactor as well as the neutron water tank. Formulation of this useful equation based on the concepts of phase space is a long mathematical step. This

Boltzmann equation for radiation transport has however been expressed in literatures as:

$$\frac{1}{v}\frac{\partial \Phi}{\partial t}(r,E,\Omega,t)+\underline{\Omega}\bullet\underline{\nabla}\Phi(r,E,\Omega,t)+\sum_t.\Phi(r,E,\Omega,t)=$$

$$\int_\Omega\int_E\sum_s(E'\rightarrow E,\Omega'\rightarrow\Omega)\Phi(r,E,\Omega,t)dE'd\Omega'+S^+(r,E,\Omega,t) \quad \text{.....5.0}$$

Where

$\frac{1}{v}\frac{\partial \Phi}{\partial t}(r,E,\Omega,t)$ -refers to the in-balance term in the equation

$\underline{\Omega}\bullet\underline{\nabla}\Phi(r,E,\Omega,t)$ - refers to the streaming term describing particles or neutrons that went through our reactor or the neutron tank without interaction.

$\sum_t.\Phi(r,E,\Omega,t)$ - referred to as the total loss term which takes care of all the reactions leading to absorption and loss of neutron from the medium.

$\int_\Omega\int_E\sum_s(E'\rightarrow E,\Omega'\rightarrow\Omega)\Phi(r,E,\Omega,t)dE'd\Omega'$ - referred to as the scattering term describing all the scattering reaction like the elastic and inelastic reaction taking place in the neutron tank by the hydrogen atom or nuclear reactor leading to direction and energy change resulting to the moderation of the neuron.

$S^+(r,E,\Omega,t)$ Referred to as the extraneous source term, which takes care of par ticle (neutron) source in the medium which includes Pu/Be(α,n) source in the neutron tank and fission, (γ n,) etc. in the reactor.

Two major methods, the deterministic and the Monte Carlo methods are used for solving the Boltzmann neutron transport equation stated above. Deterministic methods solve this equation in a numerically approximated manner everywhere throughout a modelled system, while the Monte Carlo methods model the nuclear system (almost) exactly and then solve the exact model statistically (approximately) anywhere in the modelled system. This work employed the Monte-Carlo method (MCNP) in solving this equation for the neutron transport in the neutron tank, where the source term is the Pu/Be neutron source, the scattering term the water of the tank, the absorption term is the helium gas in the detector.

2.0 Activation experiment and the theories behind it.

Activation is the conversion of a stable isotope into a radioactive isotopes resulting from the bombardment and absorption of a neutron{2}.

2.1 The Physics of thermal neutron flux activation of In-115.

Exposing the nuclei of naturally occurring In-115 to neutron irradiation from the Pu/Be source will cause them to become radioactive;

$^{115}In + {}^{1}\mathbf{n_0}$ -------> $(^{116}In)^m$ ……6.0a

In order to conserve energy, energies in form of *gamma* and *beta* radiations are released, $(^{116}In)^{m*}$ -----> $^{116}Sn + \gamma + \beta$. ……6.0b

These energy and frequency are determined by the decay scheme of the In -116 isotope and is affected only by the neutron flux at the point of irradiation and by the activation cross section of the In-115 target material and can yield information on the energy distribution of the neutrons. The reaction rate during the In-115 irradiation and activation is as expressed in{3,2}

$$(\text{Rate of Production of In-116})\ R=\phi_{th}\sigma_{act}N_T V=\phi_{th}\Sigma_{act}V \quad \text{……..……7.0}$$

where Φ_{th} – thermal neutron flux [n/m^{-2}s^{-1}], which is *nv* i.e number of the thermal neutrons and *v*, the average velocity of thermal neutrons.

σ_{act} –Microscopic activation cross section of the indium foil [m^{-2}] belonging to the most probable velocity of Maxwell-Boltzmann distribution

N_T –number of target atoms in the Indium115 foil.

As the In-115 is activated, it's equally removed simultaneously via decay by emission of gamma rays and beta particles at the rate proportional to;

Rate of decay In-116 = λN ……..……8.0

Where λ is the decay constant of In-116 sample [s^{-1}], and N is the number of radioactive nuclei present.

The rate of change of radioactive atoms during irradiation is the difference between the rates of production and

decay given as:
dN/dt = R- λN

$$\frac{dN}{dt} = \varphi_{th}\ \sigma_{act}\ N_T - \lambda N \quad \text{.....9.0}$$

If at the beginning, N =N(0), Then solving the differential equation 9.0 gives

$$N(t) = \frac{R}{\lambda}(1 - e^{-\lambda t})$$

$$A(T) = \lambda N(T) = R(1 - e^{-\lambda T}) \quad \text{..... .....10}$$

Where; λN is the rate of disintegration of the radioactive In-116 per second in Bq, i.e. activity of the activator detector. This induced activity builds up with time as shown by fig 2.0

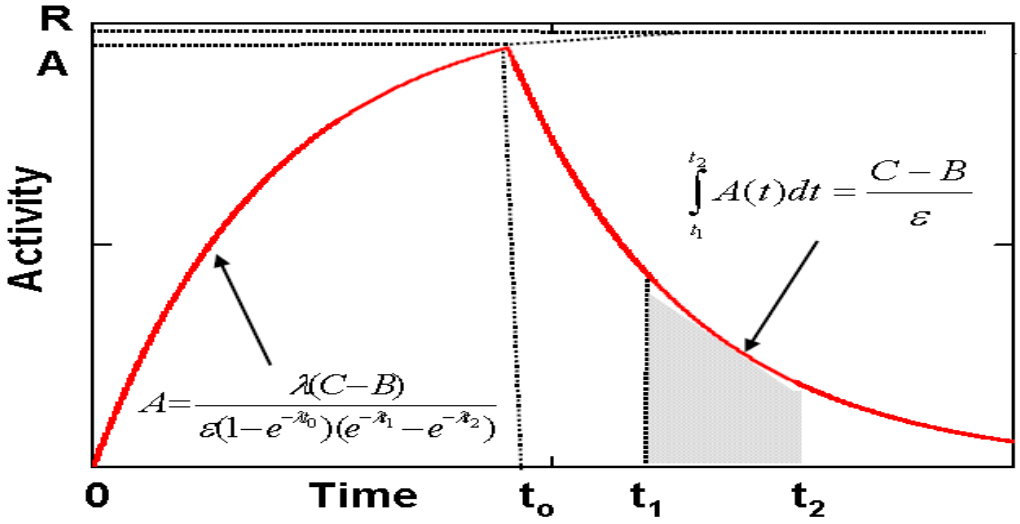

Figure 2.0 Activity of the Indium foil where t_o is the time of the foil's removal from the neutron flux. The foil's activity is counted between t_1 and t_2.
{2,3}

2.2 The Physics of determination of the thermal neutron flux from the activity of the irradiated In-116 foils

The In-116 foil transferred to an already calibrated Ge-detector is continuously decaying, an account t_o will therefore be made for the time during each step to measure the activity resulting from this exposure to the neutron flux, as shown in Figure 2.0, and the counting carried out over an interval between t_1 and t_2. The number of counts measured as presented in {3,2} will be given by

$$Count = \varepsilon \int_{t_1}^{t_2} A e^{-\lambda t} dt + B$$

$$\varepsilon \int_{t_1}^{t_2} (e^{-\lambda t_1} - e^{-\lambda t_2}) + B \quad \text{.....11.0}$$

Where ε is the overall counting efficiency and B is the background counts expected in $(t_2 - t_1)$. By combining the two equations, we obtain equation 12.0 for the saturation activity.

$$\mathbf{A} = \frac{\lambda(C-B)}{\varepsilon(1-e^{-\lambda t_0})e^{-\lambda t_0}(e^{\lambda t_1} - e^{-\lambda t_2})} \quad \textbf{.....12.0}$$

Equating $R = \phi_{th}\sigma_{act}N_T V = A$ we obtain the thermal neutron flux we are after as

$$\varphi_{th} = \frac{A_{\infty}}{N_{act}\ \sigma_{act}\ V} \quad \textbf{.....13.0}$$

$$\text{where} N_{act} = \text{no density of Indium foil} = \frac{\rho N_A (F)\%\ \text{abundance of In} - 115}{A_w\,(Atomic\,weight)} \text{ and}$$

N_A is the *Avogadro's no*; *and V* is the volume of the indium foil $= (its\,density)\,\rho$ x Mass(M)

Hence from our detector readings we could work out what the neutron flux that caused such activity in the Indium foil will be, plot this against its distance from the source point and see how these thermal neutrons are distributed in the neutron tank.

3.0 Materials used in the activation experiment:

The brief descriptions of the materials used in the activation experiments have been presented here.

***3.1 The neutron tank*:** The cylindrical tank shown on fig 3.0 contains water for shielding and thermalising and a neutron source at its centre. It's made of polyethylene wall which is also a moderator and can also be considered as a reflector. It is 113cm high and 165 cm in diameter.

Fig 3.0 snapshot of the neutron tank in Manchester laboratory used for the activation experiment.

***3.2. The sample insertion tube*:** this is the tubes that hold the indium foil for insertion into the water tank. It is 4.83cm in diameter and centred 50cm from the base and 7.5cm on either side of the source. It holds the foils in a cut open slit separated at 1.3cm from each other.

3.3. The neutron source: The Pu/Be neutron source is said to be 40 years old and with activity of 370GBq and a half-life of 24000yrs. So presently its activity will be; $A=A_o e^{-\lambda t} = 370\text{x}10^9 \text{ X } e^{-(9.149\text{E-}13\text{X } 1.26\text{E+}09)} = 369.57$GBq. It generates its neutrons through (α,n) reaction as shown in equation. Pu--α--> ($^4He_2$) + $^9Be_4$-------> $^1\mathbf{n_0}$ + $^{12}C_6$ ……...14.0

The source is enclosed in a vertical oriented cylinder 6cm high, 3cm diameter and centred 50cm above the base of the neutron tank.

3.4 The activation foil (Indium foil; In-115): This is the stable material that was made radioactive by allowing the thermal neutron present in the tank to bombard it, a sample is shown in fig4.0

Fig 4.0 One of the stable Indium-115 foil for the activation experiment (snapshot) (average measured mass of 0.0007807kg , density of 7310kg/m^3)

$In^{115} + {}^{1}n_0$ ----> $(In^{116})^{*}_{m}$ ---> $Sn^{116} \gamma + \beta$……15.0
$In^{115}(n,\gamma)In_m^{116}$; (short hand form)
This produces three key gammas, 417 keV, 1097 keV, and 1294 keV, and 1 MeV beta particle when it decays {2,5} Indium foil was selected for this experiment not only because it's readily available for laboratory testing, but also because of short half-life of 54 minute of $^{116}In_m$ allowing multiple laboratory experiments in a reasonable short period of time, and ^{115}In' has got a large thermal neutron absorption cross section of 162 barn (In-116^m ; 54min) {3}

3.5 Germanium Semi-conductor detector: The gamma ray produced during the decay of the activated In-116 was counted using this equipment (fig 5.0). Selected because it possess the highest performance among detectors with exceptional energy resolution, though requires cooling gadget containing liquid Nitrogen {6}.

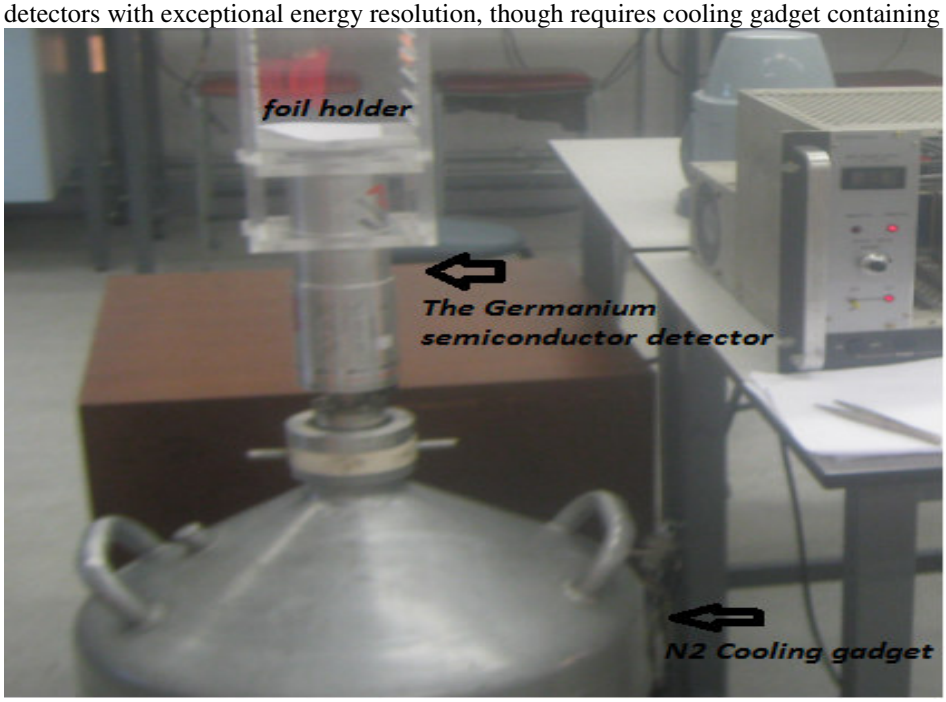

Fig 5.0 snapshot of Ge-semiconductor detector used in the experiment.

4.0 Activation experiment and the result.
To identify the energy and true count associated with each photo-peak in the irradiated In-116 samples, energy calibration of the entire counting system and the Ge- detector's efficiency was first determined. *A* counting sealed Eu-152 and Ba-133 gamma ray source was each placed on the Ge-detector and sufficient counting time of 5min was used to collect a spectrum for energy callibration. The efficiency of the Ge-detector was determined using Eu-152, a known energy source.

4.1 Gamma–ray counting of the Activated In-116
The activated In-116 at a particular noted distance from the source is taken out of the tank and time t_1 was noted down. It is then placed on the detector and acquisition time t_2 of 300secs was observed in each round of exercise for all the foils to collect enough gamma spectrums. The experimental set-up is shown on fig6.0 and one of such spectrum is shown below on fig7.0

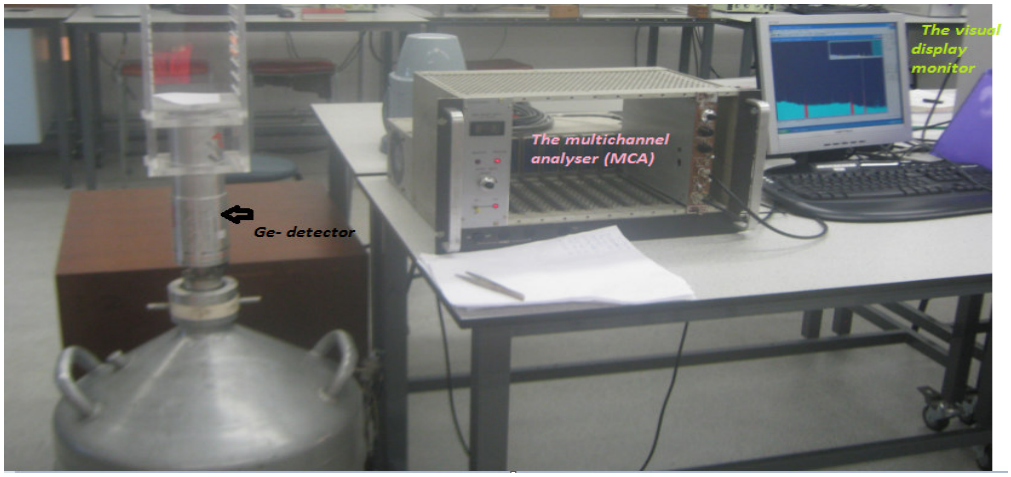

Fig6.0 The experimental set-up (Ge- detector-MCA-monitor)(snap shot)

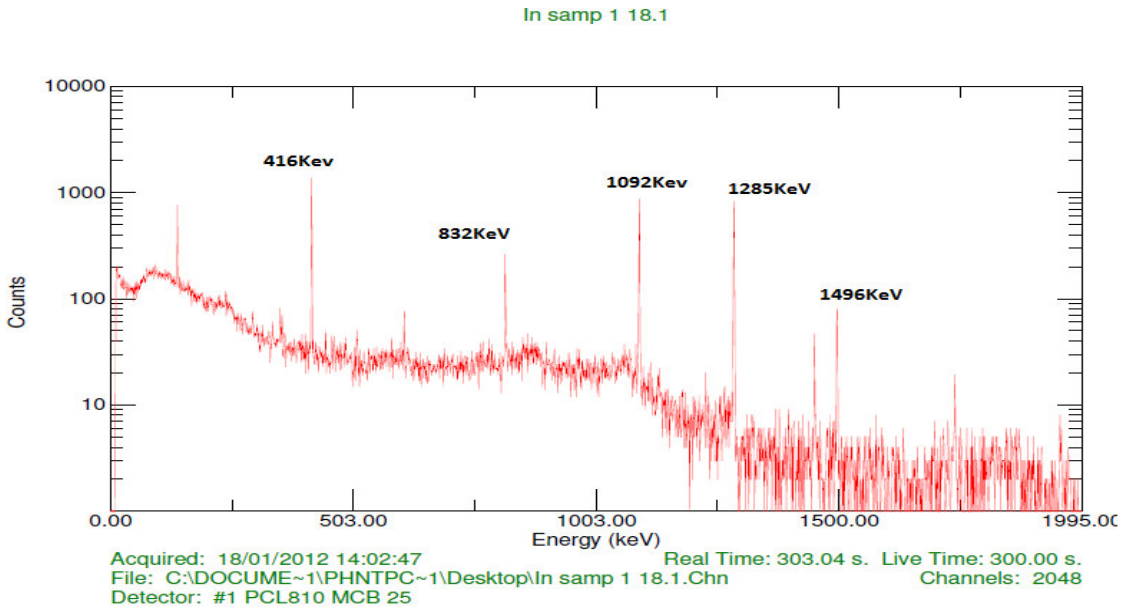

Fig 7.0 one of the collected spectrums of In-116 decay reading from the Ge-detector.

The channel number of all full energy peaks and other significant details were obtained and recorded for each round of exercise, the activity and thermal flux calculation at each distance was done with equation 13.

4.2 Plot of activity versus distance:

The graph of the activity of the In-116 versus its distance from the source was first plotted and the shape of such graph is displayed on fig.8.0 to see all the features.

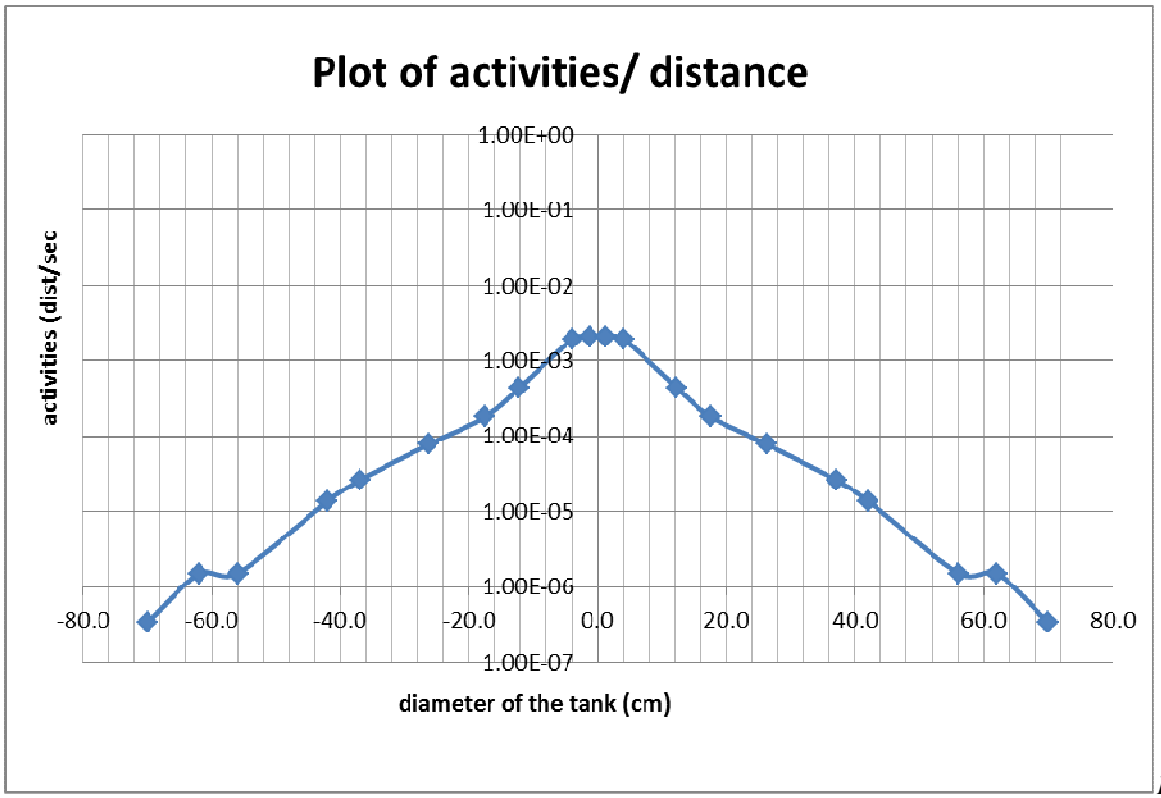

Fig8. 0: the graph of activity of the In-116 against its distance from a neutron source

The above graph shows the relationship between the activity of the In-116 foil and its distance from the neutron source. It could be easily observed that activity is maximum at the centre of the tank and diminishes towards the edge of the tank. Hence as the distance from the source increase the activity decreases.

4.3 Thermal neutron flux shape in a polythene walled tank:

The Plot of the neutron flux against distances from the source displayed the thermal neutron flux shape as shown on fig9.

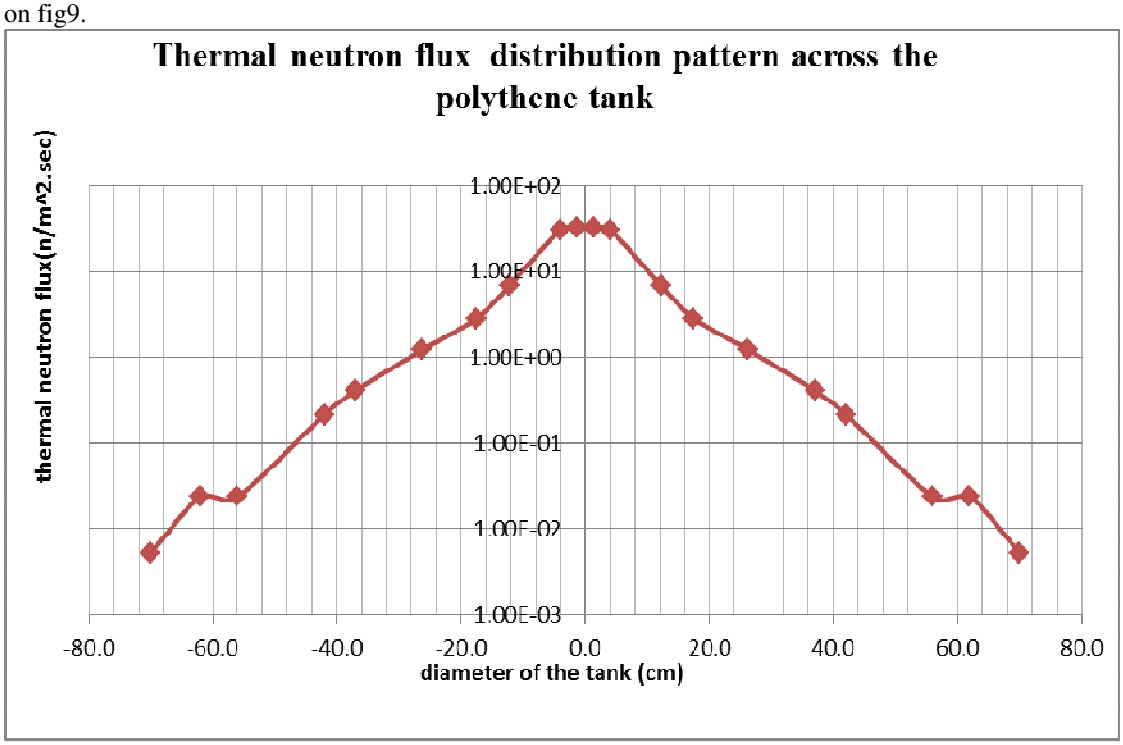

Fig9 Graph showing the distribution pattern of thermal neutron flux in the polythene wall neutron tank with the neutron source at the centre of the tank.

From this graph we could also see a unique pattern of distribution where the thermal neutron flux is maximum at the centre of the tank but decreases towards the edge of the tank obeying the Fick's theory of diffusion. Worthy to mention is the little rise in the flux level towards the edge of the polythene walled neutron tank which eventually tends to zero. This could be the polythene thermalizing fast escaping neutron and throwing them back into the tank.

5.0 MCNP SIMULATION AND THEORETICAL BACKGROUND:

MCNP version5; Monte Carlo N-Particle Transport Code System Oak ridge national laboratory managed by UT-BATTELLE, LLC for the U.S department of energy was used in this modelling. The water in the tank besides shielding effect moderate and thermalized the fast born neutron. The aim is not to obtain thermal neutron flux by activation method as done above but to use a different method to obtain the thermal flux distribution in the tank. The simulation was done with four He-3 neutron detectors (cell 10, 21, 22 and 23) (30cm high and 2.5cm diameter detector; normal length of 100cm reduced so as to get more direct impingement and avoid dividing the detectors into cells).More theories and simulation ethics could be gotten from {7,8,9} .

The Pu/Be was assumed to be a point isotropic source place at the centre of the tank. Material 1 was taken as the detector, material 2 as the water moderator and material 3 as polyethylene or stainless steel as the case may be. Four detectors was used at once so as to cover much distance within just few number of simulations, with the detectors placed at different distances at the four cardinal points inside the water tank as shown on fig 10.

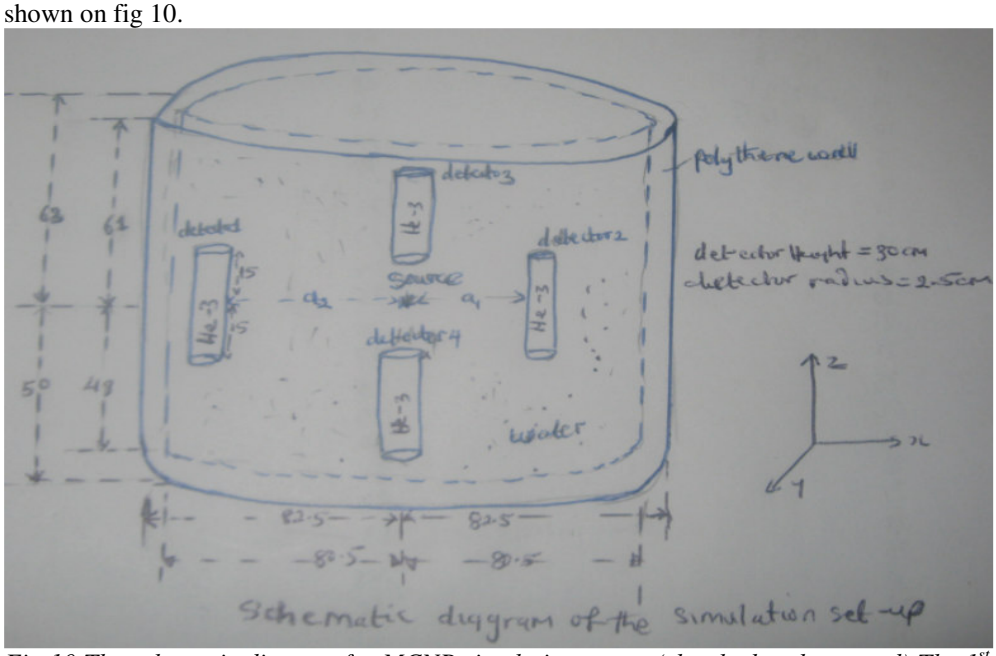

Fig 10 The schematic diagram for MCNP simulation set-up (sketched and snapped) The 1st –set-up has the wall of the tank thick and made of polyethene, while the 2nd –set-up has the wall of the tank bare and made of stainless steel.(to observe the effect of the wall type on the flux distribution pattern).

5.1 First simulation set-up*:* The wall material for this simulation set-up was made with polythene. Thermal treatment card for lwrt and for polythene was included for thermal treatment and densities as well. The geometry of this set-up as gotten from the MCNP plot window before running the programme is as shown on fig11

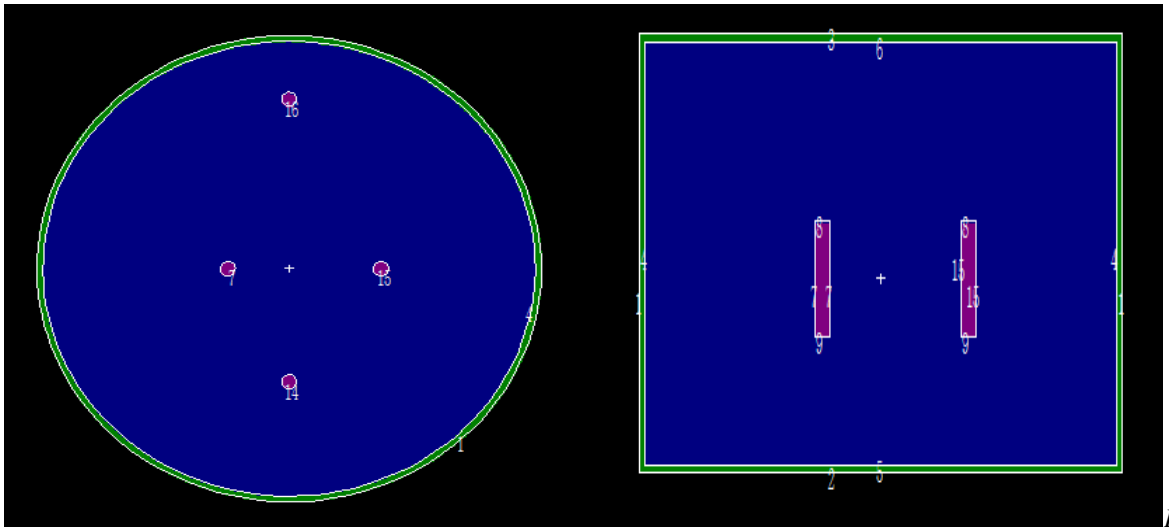

Fig1 1 The obtained Geometry from the MCNP plot window (a) in the Z direction i.e. from top and (b) in the x and y direction. (The pink object is the detector, the blue colour is the moderating water, and the green is the polythene wall.)

5.1.1 Thermal neutron flux shape in a polythene walled tank:

After running the programme, the output 'fileo' contain neutrons with different energies, but only that corresponding to the thermal energy range was picked noting the corresponding distance at which that detector was placed. The plot of this distances from the source against the flux shows the flux pattern displayed on fig12

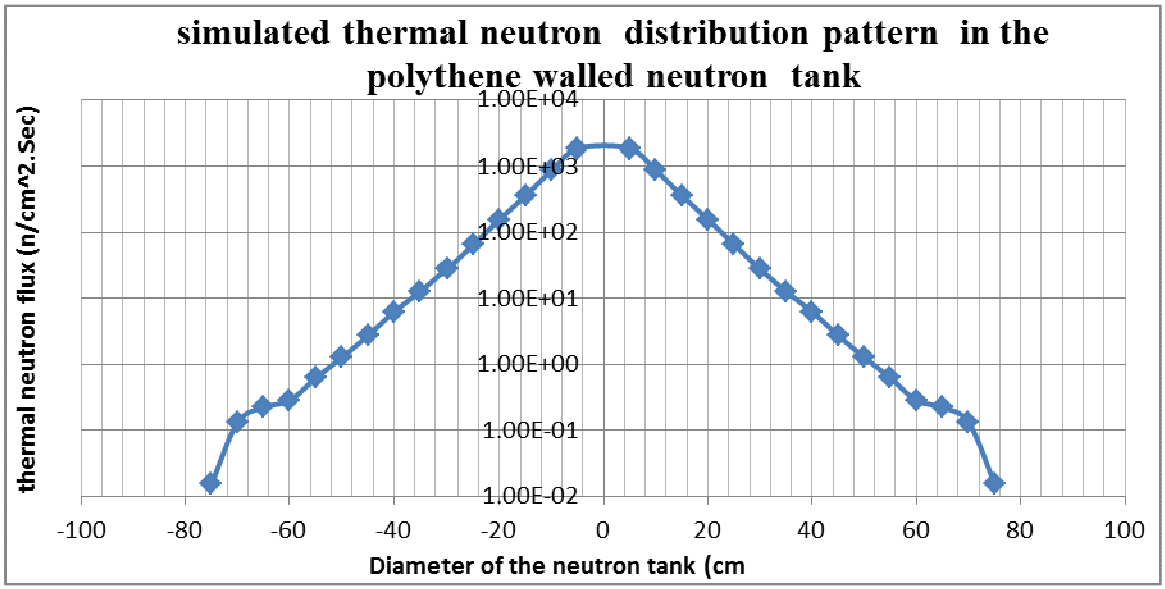

Fig 12. Simulated graph of neutron flux distribution against distance from the neutron source in the neutron tank made of polythene material.

This figure is similar to that obtained from the experiment, and shows that thermal neutron flux having a definite maximum at the centre decreases tending to zero as we move towards the edge of the tank obeying the Fick's law of diffusion. The small neutron flux rise at the end of graph equally similar to that from the experimental work can also be noticed. This could be due to the effect of the polythene wall which is also a moderator and helps in preventing the escape of some fast neutrons.

5.2 The second simulation set –up

The wall of this second set-up was made of stainless steel (chromium, nickel and iron). The thermal treatment card present in the previous set for polythene was removed, only that for water is left and densities as well. The MCNP plot of that file to check for geometry before simulation is shown on fig13

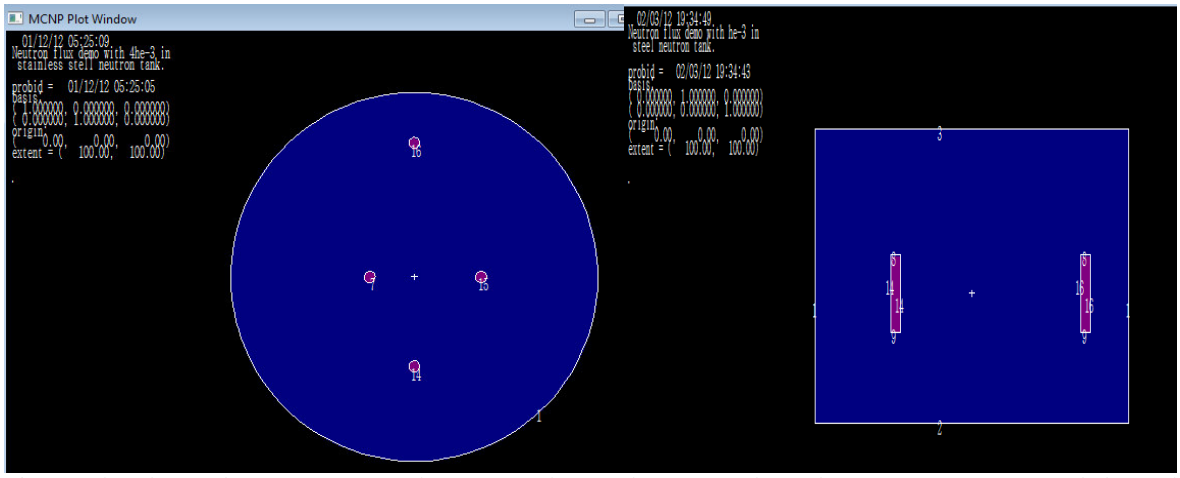

Fig 13 *The obtained Geometry from the MCNP plot window (a) in the Z direction ie from top and (b) in the x and y direction.(the pink object is the detector, the blue colour is the moderating water, and the single white line is the stainless steel wall of the tank.)*

5.2.1 Thermal neutron flux shape in a stainless stell walled tank:

The plot of neutron flux against its distance from the center was plotted and the shape of the flux is as displayed in fig14

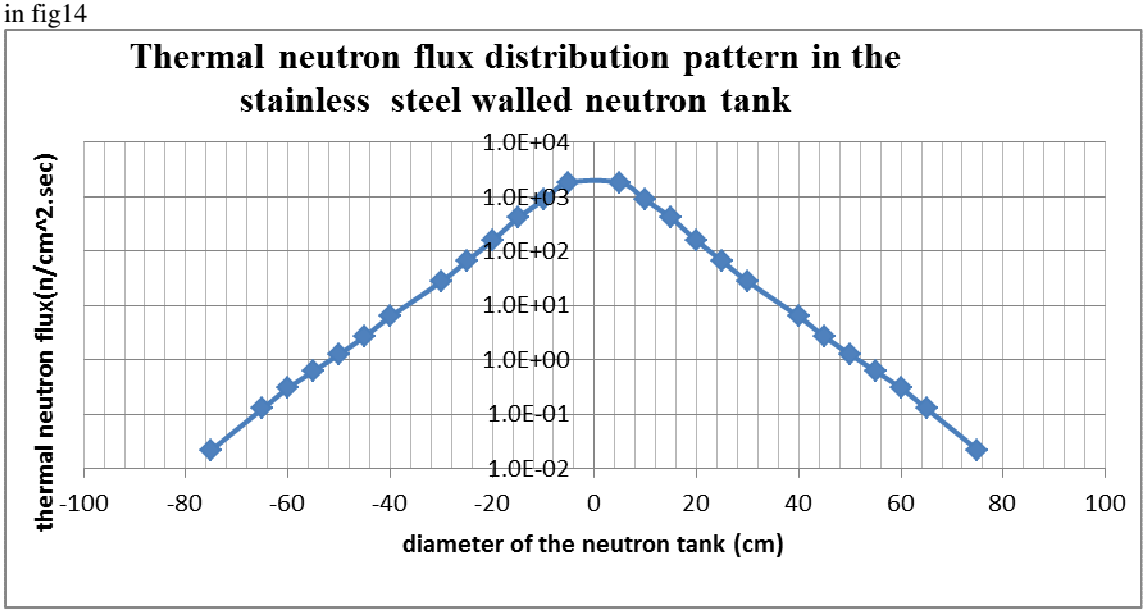

Fig 14 Simulated graph of neutron flux distribution against distance from the neutron source in the neutron tank made of stainless steel material.

The thermal neutron pattern still maintain its distribution of decreasing as we move toward the edge of the tank, however the little rise in flux as seen in the previous graphs has disappeared probably because the stainless steel cannot thermalized and reflect neutron back into the tank. It is obvious that the property of the polythene wall is different from that of the stainless steel wall. Besides having noted that activity and thermal flux are directly proportional to each other and indirectly proportional to distance from the neutron source, we could also from the curves in fig 12 and 14 observe some other important findings as have been discussed here.

6.0 DISCUSSIONS OF WALL EFFECT ON FLUX SHAPE:

The effect of the polythene wall and stainless steel wall of the neutron tank on the thermal neutron flux shape from the experiment and MCNP simulation was discussed here in these two broad headings. The physical meaning, implication and application of these results was discussed also.

6.1Flux shape in polythene wall from experiment versus MCNP simulation

The dume shape of thermal neutron flux distribution pattern obtain from the activation experiment (blue colour) and that from the MCNP simulation (red colour) in a polythene walled neutron tank have been displayed in fig15

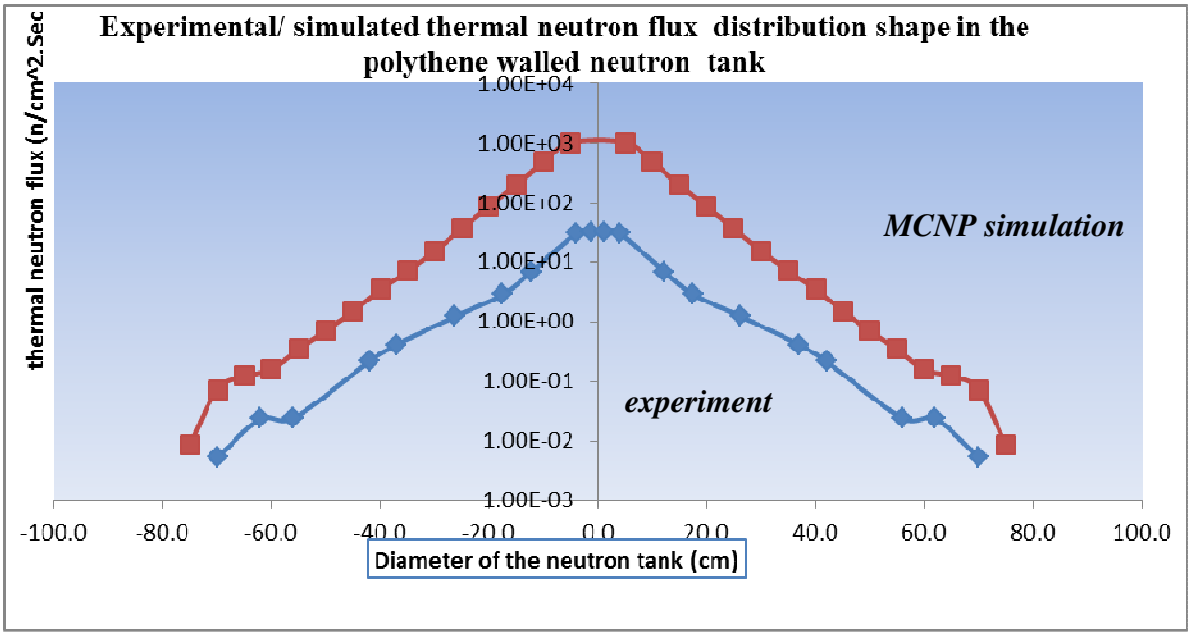

Fig15. the experimental curve and the simulated curve of neutron flux distribution pattern in the polythene walled neutron tank (maximum flux at the centre of the tank and little rise at the edges)

Thermal neutrons like gas can be seen to have moved from area of higher density to that of lower density.This is in obedience to Fick's law of neutron diffusion and has been obeyed by each of these graphs. The similarity in shape between these two different graphs involving polythene wall container is very observable. The little rise in flux at the edges before falling off to zero could be due to the thermalising effect of the polythene.This shape is analogous to what is obtainable in a nuclear reactor with a reflector. The implication of this in a thermal reactor is that the reactors without reflector will produce little power at the edged compared to the center since the thermal neutron flux is proportional to reactor power. The flux has very definite maximum, and at the center of the tank, again equivalent to the reactor core, the implication of this distribution in thermal reactor is that maximum power will be produced by nuclear fuel near the center of the core, hence they burn out faster than those at the edges which is the cause of the differential burning in reactor and economic wastage. However the use of differential enrichment is used to ameliorate this effect, or using a reflector. Fuels at the edges could be enriched lower because the thermal flux distribution has shown that they have fewer thermal neutrons there, and those at the center higher, because of the high thermal neutron flux shown by the distribution curve. These have been made possible because of the revelation gotten from studying thermal neutron flux distribution pattern in the reactor core as done in this work.

6.2 Flux shape in polythene wall versus stainless steel wall

Comparison and the difference between the flux pattern from the two MCNP simulation set ups with polythene and steel wall is displayed on fig16.

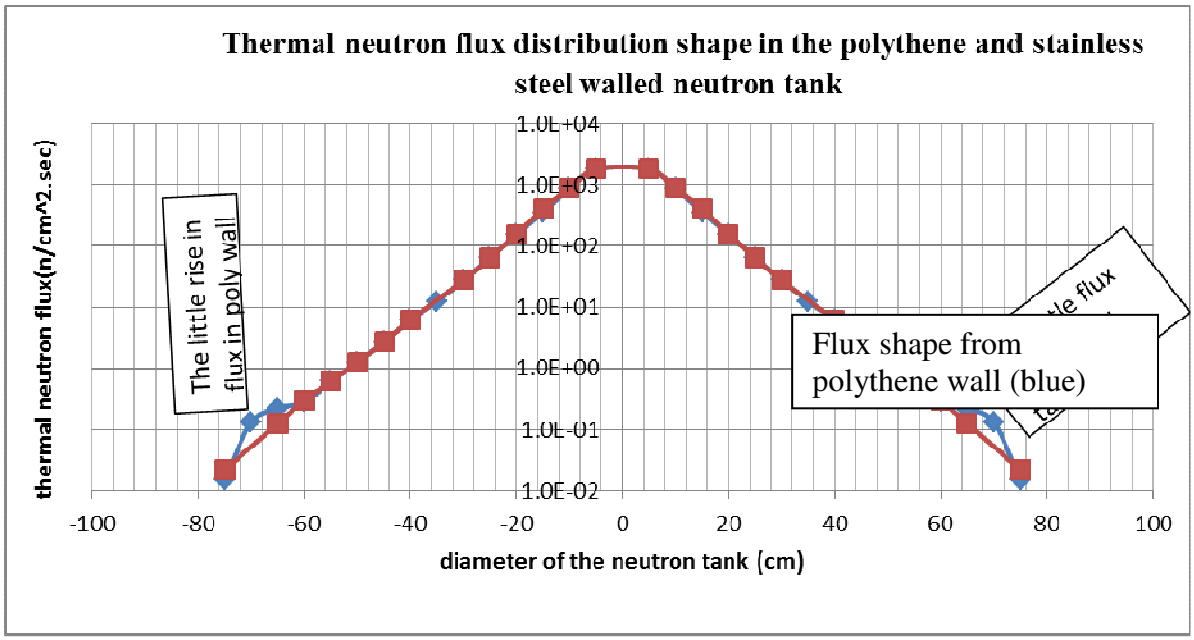

Fig 16 The effect of wall material (polythen and stainless steel) on thermal flux pattern.

we could see obviously the effect of these material on the flux pattern, with the stainless behaving like bare reactor core and the polythen could be likened to a reflected reactor core. The polythene which is a good neutron moderator is acting a little like a reflector; a reflector is a material with moderating properties placed around a reactor core to reflect neutrons back into core for more fission. We could observe a little rise in thermal neutron flux which means little power rise if it's in a reactor. The flux near the edge rises a little about 10% of the maximum flux before dropping off finally to zero. This isn't same with stainless steel walled graph, because the steel has no moderating properties. The flux still retains maximum value at the center in each case, but the average flux may have risen to about 40% in the reflected core when both the axial and radial distribution of flux is accounted for. From what we have known, we could then say that having a reflector round the reactor is a good idea, the implication of a reactor without it is that thermal neutron flux distribution seen in the stainless stell walled tank equivalent to that seen in bare reactors will lead to

- Poor use of fuel in the outer region of the core to produce power
- Differential burning of fuel
- Limitations of total power produced because of high ratio of the maximum flux to average flux

Most reactors have reflectors, AGR is said to have a graphite reflector around its core, and its presence leads to decrease of the linear dimensions of the critical reactor. Conclusively, thermal neutron spectrum has been shown to be high at the center of the core with definite maximum and flattens out to zero, as distance from the source increases towards the edge because of neutron diffusion effect and same has been shown to happen in the neutron tank. The experimental and simulation results coincided with theoretical predictions mentioned in the body of the work.

7.0 Acknowledgements:
I wish to acknowledge the staff and personnels of school of Physics and Astronomy and the Schuster Laboratory University of Manchester for providing these necessary expensive equipments, materials and softwares for this work. I wish to also acknowledge TETFUND Nigeria (Tertiary Education Frust Fund) who funded me through Nnamdi Azikwe University Awka, Nigeria. I am equally grateful to Nnamdi Azikiwe University Awka Anambra State, Nigeria for their all-round support.

8.0 REFERENCES:

{1}Samuel, G. and Alexander, S; 1981: Nuclear reactor engineering, Van Nostrand Reinhold ltd New York N.Y 10020; PP13- 200
{2}Stephanie Vaughn, BS, 2003. investigation of a passive, temporal, neutron monitoring system that functions within the confines of start i; MSc (Nuclear Science) THESIS Presented to the Faculty Department of Engineering Physics Graduate School of Engineering Management Air Force Institute of Technology Air University,USA; AFIT/GNE/ENP/03-10.http://www.dtic.mil/cgi-bin/GetTRDoc?AD=ADA412872
{3} Glenn F. Knoll, 2000. Radiation detection and measurements; third edition; John Wiley and sons Inc. *pp 744-749*

{4}Weston M. Stacey,2007; Nuclear Reactor Physics, Second Edition, Completely WILEY-VCH Verlag GmbH & Co. KGaA, Weinheim
{5} Glascock, Michael D, 1985. Neutron Activation Analysis Tables University of Missouri: Research Reactor Facility. July.
{6} Kenneth, J.S and Richard E. F, 2008. Fundamentals' of nuclear Science and Engineering 2nd edition, CRC press Taylor & Francis Group Boca Raton p194
{7} Andrew Boston; 2000. Introduction to MCNP-the Monte Carlo transport code Olive Lodge Laboratory
{8} X-5 Monte Carlo Team, 2003; MCNP — A General Monte Carlo N-Particle Transport Code, Version 5, Volume II: User's Guide, Los Alamos Controlled Publication; distribution is limited, LA-CP-03-0245
{9} Oak Ridge National Laboratory 1966, Radiation Shielding and Information Center, Report 10, Oak Ridge, TN.

The IISTE is a pioneer in the Open-Access hosting service and academic event management. The aim of the firm is Accelerating Global Knowledge Sharing.

More information about the firm can be found on the homepage:
http://www.iiste.org

CALL FOR JOURNAL PAPERS

There are more than 30 peer-reviewed academic journals hosted under the hosting platform.

Prospective authors of journals can find the submission instruction on the following page: http://www.iiste.org/journals/ All the journals articles are available online to the readers all over the world without financial, legal, or technical barriers other than those inseparable from gaining access to the internet itself. Paper version of the journals is also available upon request of readers and authors.

MORE RESOURCES

Book publication information: http://www.iiste.org/book/

Academic conference: http://www.iiste.org/conference/upcoming-conferences-call-for-paper/

IISTE Knowledge Sharing Partners

EBSCO, Index Copernicus, Ulrich's Periodicals Directory, JournalTOCS, PKP Open Archives Harvester, Bielefeld Academic Search Engine, Elektronische Zeitschriftenbibliothek EZB, Open J-Gate, OCLC WorldCat, Universe Digtial Library , NewJour, Google Scholar